



■ HIP

# Osseointegration of retrieved 3D-printed, off-the-shelf acetabular implants

**L. Dall'Ava,  
H. Hothi,  
J. Henckel,  
A. Di Laura,  
R. Tirabosco,  
A. Eskelinen,  
J. Skinner,  
A. Hart**

From University College London (UCL) - Stanmore Campus (Royal National Orthopaedic Hospital), Stanmore, UK

**Aims**

The main advantage of 3D-printed, off-the-shelf acetabular implants is the potential to promote enhanced bony fixation due to their controllable porous structure. In this study we investigated the extent of osseointegration in retrieved 3D-printed acetabular implants.

**Methods**

We compared two groups, one made via 3D-printing (n = 7) and the other using conventional techniques (n = 7). We collected implant details, type of surgery and removal technique, patient demographics, and clinical history. Bone integration was assessed by macroscopic visual analysis, followed by sectioning to allow undecalcified histology on eight sections (~200 µm) for each implant. The outcome measures considered were area of bone attachment (%), extent of bone ingrowth (%), bone-implant contact (%), and depth of ingrowth (%), and these were quantified using a line-intercept method.

**Results**

The two groups were matched for patient sex, age (61 and 63 years), time to revision (30 and 41 months), implant size (54 mm and 52 mm), and porosity (72% and 60%) (p > 0.152). There was no difference in visual bony attachment (p = 0.209). Histological analysis showed greater bone ingrowth in 3D-printed implants (p < 0.001), with mean bone attachment of 63% (SD 28%) and 37% (SD 20%), respectively. This was observed for all the outcome measures.

**Conclusion**

This was the first study to investigate osseointegration in retrieved 3D-printed acetabular implants. Greater bone ingrowth was found in 3D-printed implants, suggesting that better osseointegration can be achieved. However, the influence of specific surgeon, implant, and patient factors needs to be considered.

**Cite this article:** *Bone Joint Res* 2021;10(7):388–400.

**Keywords:** 3D-printing, Additive manufacturing, Osseointegration, Hip arthroplasty, Retrieval analysis

**Article focus**

- Assessment of osseointegration of retrieved, 3D-printed, off-the-shelf acetabular implants.
- Comparison with conventionally manufactured, off-the-shelf acetabular implants.

- Consistent presence of lamellar bone in 3D-printed implants.

**Strengths and limitations**

- First study to investigate the osseointegration of 3D-printed acetabular implants retrieved from patients.
- Small number of implants and influence of surgeon, patient, and implant factors on the osseointegration outcomes.

**Key messages**

- 3D-printed implants showed higher degree of osseointegration compared to conventional implants.

Correspondence should be sent to Lorenzo Dall'Ava; email: [lorenzo.dallava.17@ucl.ac.uk](mailto:lorenzo.dallava.17@ucl.ac.uk)

doi: 10.1302/2046-3758.107.BJR-2020-0462.R1

*Bone Joint Res* 2021;10(7):388–400.

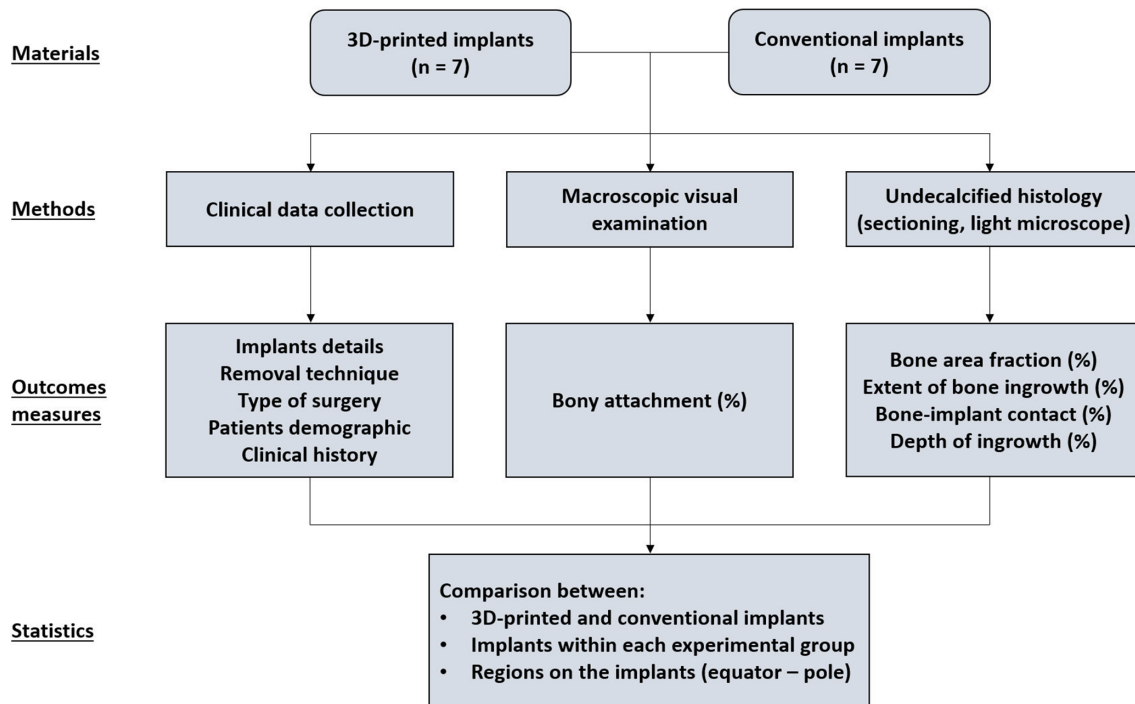


Fig. 1

Flow diagram summarizing the design of the study.

## Introduction

The past decade has seen a sharp increase in the use of additive manufactured (AM) (also known as 3D-printed) orthopaedic implants, primarily off-the-shelf (i.e. not patient-specific) acetabular implants for total hip arthroplasty (THA). In the UK in 2018, 13% of the uncemented acetabular implants used in revision surgeries were 3D-printed.<sup>1,2</sup>

Aseptic implant loosening is still the most common reason for revision and re-revision in THA using conventionally manufactured implants.<sup>1</sup> 3D-printed implants aim to avoid this by enhanced fixation with the host bone, due to a higher coefficient of friction against bone for increased initial stability and a highly porous structure similar to that of bone tissue.<sup>1-4</sup> Recent studies have shown satisfactory clinical outcomes of highly porous acetabular implants in the short- and mid-term, however long-term results are yet to be published.<sup>2,5</sup>

Despite several *in vitro* and *in vivo* (animal) studies having shown good osseointegration properties of 3D-printed scaffolds and structures for potential orthopaedic applications,<sup>6-12</sup> human studies are lacking and poorly understood<sup>13</sup> because of the limited number of retrieval analyses.<sup>14-17</sup> Furthermore, studies including highly porous orthopaedic implants are mainly focused on testing the primary stability,<sup>18,19</sup> and there is no study of human osseointegration of retrieved 3D-printed implants.

We aimed to compare bone integration of retrieved, off-the-shelf acetabular implants made by either 3D-printing or conventional methods. We used visual

scoring and histological analysis of retrieved implant sections. Our null hypothesis was that the manufacturing method (3D-printing or conventional) had no effect on implant-bone integration.

## Methods

We designed a retrieval study (Figure 1) and obtained institutional review board approval (London-Riverside REC 07/Q0401/25) and informed patient consent for each implant.

**Materials and clinical data collection.** This retrieval study included consecutively collected 3D-printed and conventionally manufactured uncemented acetabular implants with a highly porous backside surface layer (i.e. porosity > 60% and/or pore size > 400  $\mu\text{m}$ )<sup>5,20</sup> received at our centre between September 2013 and September 2019, following removal at revision. Of the 3,000 implants collected, 14 retrieved acetabular implants met the criteria. The implants were divided into two groups according to the manufacturing method: 3D-printed ( $n = 7$ ) and conventionally manufactured ( $n = 7$ ) (Figure 2).

We collected implant details (diameter, morphometric features of the porous structures, type of bearing surfaces, reason for revision, time to revision), the removal technique (explant tool used or not), the type of surgery (primary or revision), patient demographic (sex, age at surgery), and clinical history.

The design of the 3D-printed implants consisted of the uncemented off-the-shelf Delta TT ( $n = 6$ ) and Delta ONE TT cups ( $n = 1$ ) (LimaCorporate, Italy), which were produced by electron beam melting (EBM), as



Fig. 2

Image showing backside and internal surface of the retrieved acetabular implants, divided into 3D-printed and conventional.

3D-printing technique, using titanium-aluminium-vanadium (Ti-6Al-4V) alloy powder. The conventionally manufactured designs consisted of the uncemented off-the-shelf Trident I Tritanium (Stryker, USA), R3 Stiktite (Smith & Nephew, USA), and Pinnacle Gription (DePuy Synthes, USA), which were made of Ti-6Al-4V. A fourth design, Continuum Trabecular Metal (Zimmer Biomet, USA), was also present and this was made of tantalum (metal heavier than titanium). The dense solid wall (dome) of the conventional acetabular implants had been manufactured by computer numerical controlled (CNC) machining, while the porous structures present on the backside surface of these implants had been made by specific techniques for porous metal fabrication. The Tritanium porous structure had been made by depositing commercially pure titanium powder on a sacrificial porous polyurethane scaffold via physical vapour deposition, and sintering at high temperature the resulting porous metallic structure onto the machined implant dome.<sup>21</sup> The Stiktite porous structure had been made by sintering asymmetrical Ti-6Al-4V powder on the acetabular dome at high temperature. The Gription porous structure had been fabricated by sintering both spherical beads and irregular particles made of commercially pure titanium onto the implant dome. The Trabecular Metal structure had been made by depositing commercially pure tantalum on a polymer foam skeleton via chemical vapour deposition, and subsequently sintering onto the acetabular dome.

**Macroscopic visual examination.** A photogrammetric method was used to assess the area of bony attachment (ingrowth) on the acetabular implants. This method included an imaging system (EOS 5D Mark II camera; Canon, Japan) and a public domain software for image analysis (ImageJ 1.52a; National Institutes of Health, USA), positioning a reference scale in the field of view for image calibration.

The implants were divided into quadrants and sub-quadrants, according to the region (pole or equator), following a previously published method.<sup>22</sup> Bony attachment was calculated for the whole quadrants and specific

sub-quadrants (pole or equator). Both the overall and sub-quadrant results were compared within and between the two groups.

**Bone ingrowth.** The acetabular implants were prepared for undecalcified histological analysis. The preparation involved dehydration in solutions of ascending concentration (70%, 90%, two steps at 100%) of industrial methylated spirit (Solmedia, UK) in distilled water, infiltration in alcohol-resin solution (ratio 1:1), and embedding in hard grade acrylic resin 100% (London Resin (LR) White; Agar Scientific, UK). The resin polymerization was initiated by the addition of a catalyst at room temperature (LR White Accelerator; Agar Scientific). Eight thin sections (~200 µm) passing through the hole for screw insertion located at the pole were obtained from each implant (Figure 3), using a water-cooled diamond-coated band saw and a grinding machine (EXAKT Advanced Technologies, Germany). The sections were subsequently stained with Toluidine Blue (soft-tissue) and Paragon (bone). All the preparation steps were carried out following previously published standard operating procedures for histological evaluation of specimens after impregnation and casting in hard grade acrylic resin.<sup>23</sup>

**Analysis of bone ingrowth.** The sections were imaged using an optical light microscope (Keyence VHX-700F; Keyence Co., Japan) at a magnification of 50×. Eight images were taken for each section (Figure 3), resulting in 64 images for each implant. Each section was also divided into two regions (equator and pole), adapting the DeLee-Charnley zones.<sup>24</sup>

A line intercept method was employed to quantify bone ingrowth within each histological image. A mask of interconnecting lines measuring 5.4 mm × 1.1 mm was superimposed over each image (around 150 intersecting points per image), and the type of material at the intersection of each line was recorded (bone, metal, or neither of these) (Figure 4). The analysis method applied in this study was adapted from previously published works.<sup>15,23</sup> Overall, a total of around 230,000 data points were collected.

The bone ingrowth analysis consisted of four outcome measures: 1) bone area (BA) fraction: fraction of available

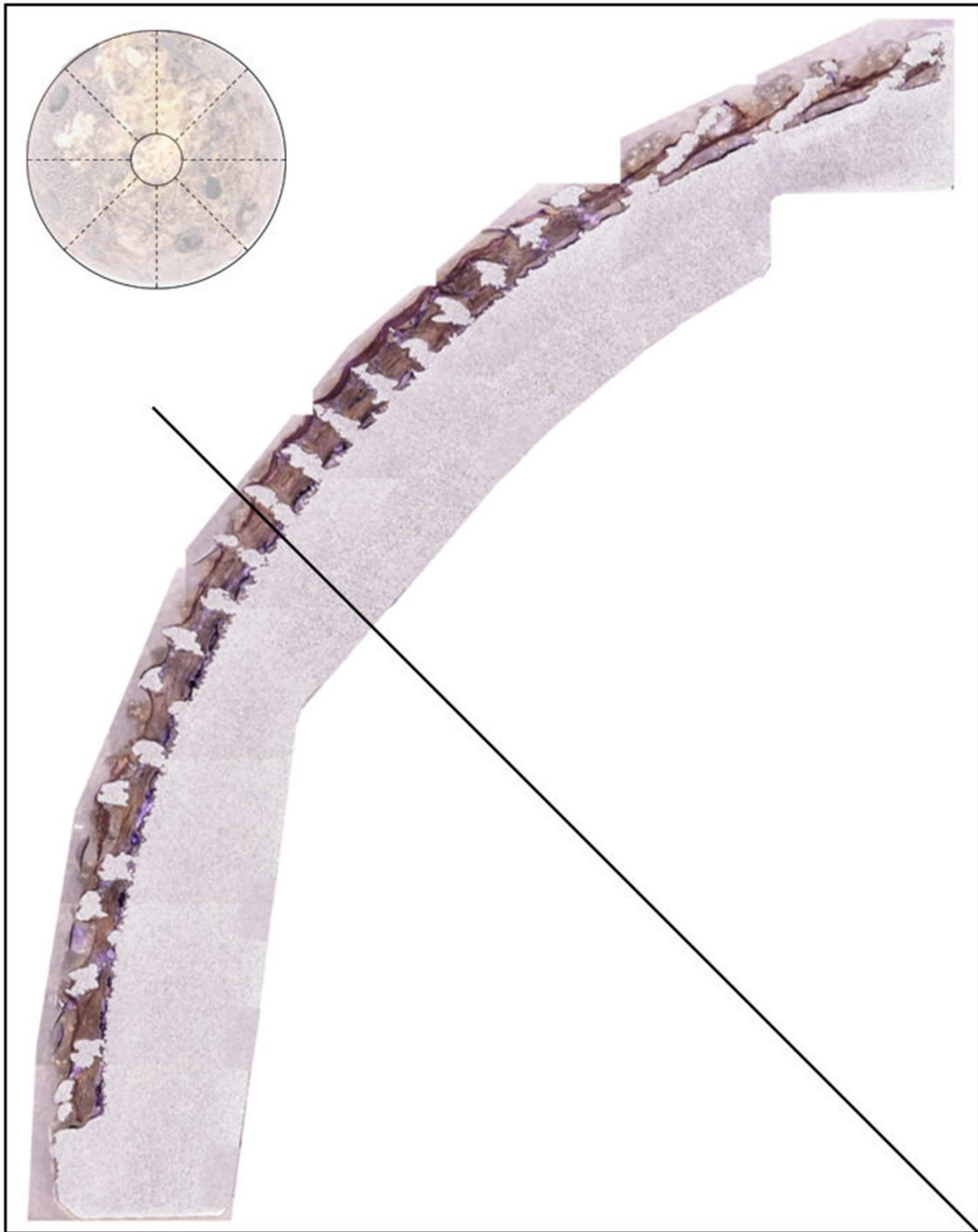


**Fig. 3**

Image showing the schematic location of the eight sections obtained from an implant, and a representative section (the eight images were stitched together) with the line separating the pole (top right) and the equator (bottom left) regions (staining: Toluidine Blue, Paragon; magnification 50 $\times$ ).

porous space occupied by bone, expressed as percentage, and providing a volumetric indication of ingrowth; 2) extent of ingrowth: calculated by dividing each image into sectors (using the same mask of interconnecting lines) and by measuring the fraction of sectors in which bone tissue was present, expressed as percentage of the total number of sectors (Figure 4). It provides a topological

indication of the distribution of ingrowth across the back-side surface of the acetabular implant; 3) bone-implant contact (BIC): calculated as the percentage of points where the lines of the grid intersected directly with bone and metal without any space in between the two. If BIC exists, it provides an indication of good osseointegration without fibrous tissue inserted in this interface zone; and

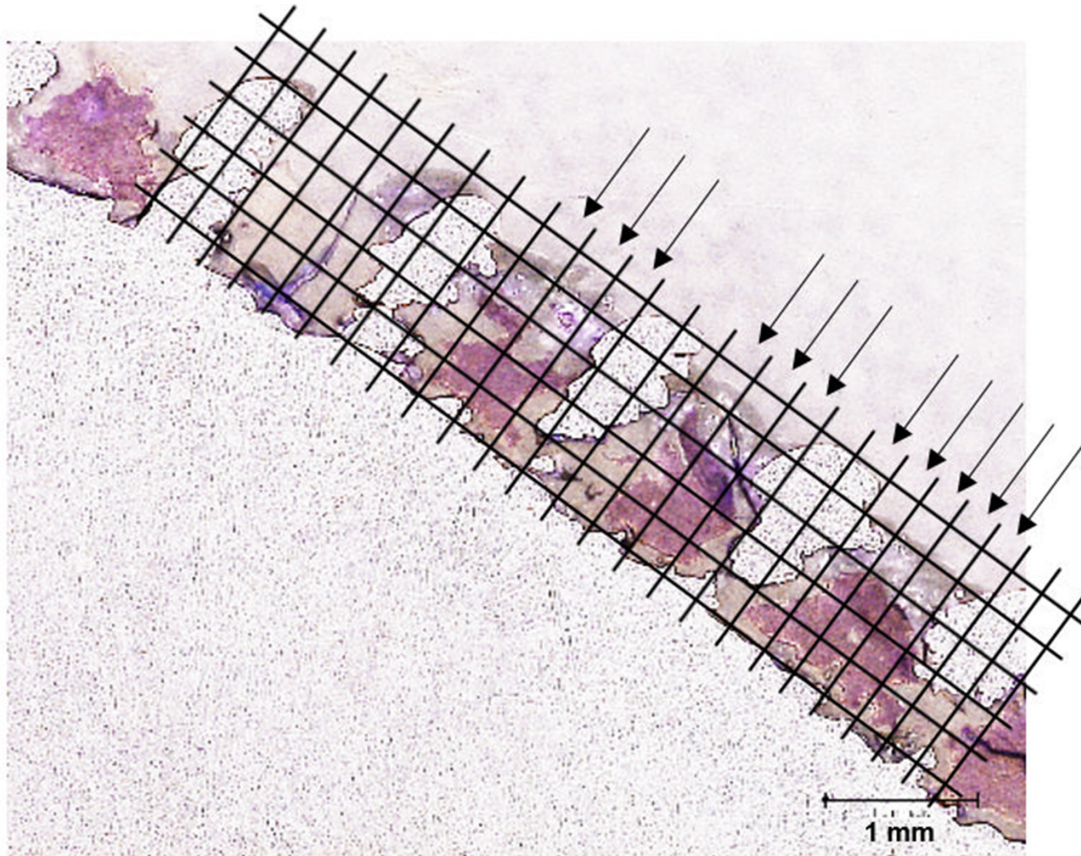


Fig. 4

Image showing a representative example of the outcome measures considered in the study, with the mask of interconnecting lines superimposed to one of the images taken from a histological section. Bone area was calculated using the grid, and the black arrows indicate the sectors with presence of bony tissue (staining: Toluidine Blue, Paragon; magnification 50 $\times$ ).

4) depth of ingrowth: defined by calculating two parameters. First, the extent of maximum depth reached by bone was measured: this is the fraction of sectors, expressed as percentage of the total number of sectors, where bone occupied the whole thickness of the porous structure on the backside of the implants and provided an indication of the distribution across the surface. Second, the mean deepest point reached by bone in those sectors where it did not reach the maximum depth was calculated.

Overall comparison between the two groups and within each group, comparison between regions (pole and equator) within each group, and comparison of corresponding regions between groups were performed. **Statistical analysis.** Statistical analysis was performed using the statistical software package Prism (version 7.01; GraphPad, USA). All continuous variables were expressed as median (interquartile range (IQR)). The data were assessed for normality using the D'Agostino-Pearson test. Comparisons between the two groups and between the two regions on the implant (pole–equator) were performed using Mann-Whitney U tests. Non-parametric Kruskal-Wallis test with post hoc Dunn's correction

was used for comparison within each individual group. Fisher's exact test was carried out to compare categorical variables. The level of significance for all statistical analyses was  $p < 0.05$ .

## Results

**Design features and clinical data.** A summary of the design features and clinical data related to the acetabular implants is reported in Table I. There was no statistically significant difference in patient age, sex, implant diameter, porosity, and time to revision between the two groups. All the well-fixed cups and one of the loose cups were removed using an 'explant tool', while one loose cup was removed without it. The pore size of the 3D-printed implants was significantly higher ( $p = 0.003$ , Mann-Whitney U test), and the porous structure layer on the backside surface was significantly thicker than conventional implants ( $p < 0.001$ , Mann-Whitney U test). The spread of values for the conventional group was wider because one of the implants, specifically the Continuum Trabecular Metal, showed the thickest porous structure, with a median value of 1.906 mm (IQR 1.826 to 2.007).

**Table I.** Summary of the design features and clinical data related to the 3D-printed and conventional groups.

Variable	3D-printed	Conventional	p-value
Median age, yrs (IQR)	61.1 (48.4 to 70.9)	66.0 (56.9 to 68.9)	0.999*
Sex, male, % (n)	29 (2)	57 (4)	0.592†
Median time to revision, mths (IQR)	24.9 (20.5 to 45.6)	46.3 (34.7 to 49.1)	0.366*
Median implant diameter, mm (IQR)	54 (50 to 58)	53 (50 to 56)	0.512*
Median porosity, % (IQR)	72.4 (70.8 to 74.4)	59.6 (55.7 to 71.5)	0.152*
Median pore size, mm (IQR)	0.84 (0.83 to 0.89)	0.36 (0.23 to 0.52)	0.003*
Median thickness of porous layer, mm (IQR)	1.30 (1.23 to 1.38)	1.05 (0.95 to 1.63)	< 0.001*

\*Mann-Whitney U test.

†Fisher's exact test.

IQR, interquartile range.

**Table II.** Clinical data related to each 3D-printed and conventional acetabular implant.

Case no.	Design	Diameter, mm	Bearings (head – liner)	Reason for revision	Time to revision, mths	Type of surgery	Sex	Patient age, yrs
<b>3D-printed</b>								
1	Delta TT	54	ceramic – PE	Unexplained pain	20.5	Revision	M	60
2	Delta TT	54	metal – ceramic	Unexplained pain	21.3	Revision	F	61
3	Delta TT	50	ceramic – metal	Infection	50.1	Revision	F	48
4	Delta TT	58	metal – PE	Aseptic loosening	45.6	Revision	F	71
5	Delta ONE TT	50	ceramic – PE	Aseptic loosening	24.9	Revision	F	74
6	Delta TT	56	N/A – PE	Unexplained pain	30.2	Revision	F	48
7	Delta TT	62	ceramic – PE	Underlying pelvic discontinuity	16.8	Revision	M	67
<b>Conventional</b>								
8	Trident I Tritanium	44	metal – N/A	Recurrent dislocation	49.7	Primary	M	69
9	R3 Stiktite	54	metal - metal	Unexplained pain	48.8	Primary	F	68
10	R3 Stiktite	52	metal - metal	Unexplained pain	48.9	Primary	F	64
11	R3 Stiktite	56	metal - metal	Unexplained pain	43.7	Primary	M	69
12	R3 Stiktite	52	metal - metal	Unexplained pain	43.1	Primary	F	60
13	Pinnacle Gription	54	ceramic - PE	Painful hip	43.3	Revision	M	76
14	Continuum TM	56	N/A - PE	Infection	9.5	Revision	M	48

N/A, not available; PE, polyethylene; TM, trabecular metal.

The values related to the morphometric features of the porous structure of the implants had been either measured in previous studies by micro-CT analysis,<sup>25,26</sup> measured from the sections of the implants using the software for image analysis, ImageJ (version 1.52a), or obtained from the specifications reported by the manufacturers.

Clinical data related to each individual acetabular implant are reported in Table II.

**Visual bony attachment.** The visual assessment revealed no statistically significant difference in overall bony attachment between the 3D-printed and conventional groups ( $p = 0.201$ , Mann-Whitney U test), with median values of 85.3% (IQR 23.4% to 93.8%) and 71.9% (IQR 69.6% to 78.2%), respectively. Similarly, no significant difference was found between the polar and equatorial regions both within the 3D-printed ( $p = 0.999$ ) and conventional groups ( $p = 0.456$ , both Mann-Whitney U test), and between corresponding regions of the two groups (polar:  $p = 0.902$ ; equator:  $p = 0.259$ ; both Mann-Whitney U test). The median values were 78.4% (IQR 24.5% to 97.5%), 87.9% (IQR 22.9% to 91.9%), 76.3%

(IQR 63.3% to 91.2%), and 70.9% (IQR 57.2% to 76.8%) for the polar and equatorial regions of the 3D-printed and conventional groups, respectively.

**Bone ingrowth.** The analysis of histological sections revealed statistically significant differences between the two groups in terms of overall BA, extent of ingrowth, BIC, and depth of ingrowth ( $p < 0.001$ , Mann-Whitney U test), with higher values shown by the 3D-printed group. The 3D-printed implants showed a consistently higher formation of bone within the porous structure, both in terms of volumetric presence within the available space for ingrowth and spread (extent) across the surface of the implants. Furthermore, BIC was observed to be more prevalent in the 3D-printed implants, suggesting a good degree of osseointegration.

In the 3D-printed group, bone growth also reached the maximum depth in a more uniformly distributed way than in the conventional group, and when this was not reached, then the mean point reached by bone into the porous layer was still deeper in the 3D-printed implants. A summary of the values measured for the bone ingrowth

**Table III.** Values of the bone ingrowth parameters calculated for the two groups.

Parameter	3D-printed	Conventional	p-value*
Median bone area, % (IQR)	65.7 (36.4 to 90.6)	33.9 (21.9 to 50.0)	< 0.001
Median extent of ingrowth, % (IQR)	100 (86.0 to 100)	80.9 (56.1 to 100)	< 0.001
Median BIC, % (IQR)	58.8 (17.1 to 94.2)	20.0 (10.4 to 32.4)	< 0.001
<b>Depth of ingrowth</b>			
Median extent of max depth, % (IQR)	60.0 (0 to 96.3)	5.7 (0 to 30.5)	< 0.001
Median deepest point, % (IQR)	81.8 (71.4 to 89.3)	59.5 (32.7 to 80.6)	< 0.001

\*Mann-Whitney U test.

BIC, bone-implant contact; IQR, interquartile range.

parameters related to the two groups is reported in Table III, and the distribution of the values of BA is shown in Figure 5a.

Presence of lamellar bone structures could be observed in some histological sections obtained from the 3D-printed implants (at least in four of the seven implants analyzed), while this was not clearly observed in the conventional group (visible in only one implant of the seven analyzed) (Figure 6). The lamellar structures are depicted by the darker lines within bone tissue arranged according to the closest surface. Representative images of high, medium, and low percentage of bone ingrowth in a 3D-printed and conventional acetabular implant are shown in Figure 7.

The comparison of bone ingrowth parameters between the equator and pole regions of the 3D-printed implants revealed no significant differences in terms of BA ( $p = 0.984$ ), extent of ingrowth ( $p = 0.358$ ), BIC ( $p = 0.509$ ), and extent of maximum depth ( $p = 0.619$ , all Mann-Whitney U test). However, a significant difference was present between the regions in terms of median deepest point reached by bone when the maximum depth was not reached ( $p < 0.001$ , Mann-Whitney U test), with higher values shown in the histological images obtained from the equator of the implants. The median values were 66.2% (IQR 36.8% to 89.8%) and 65.0% (IQR 36.1% to 91.9%), 100% (IQR 86.4% to 100%) and 100% (IQR 85.2% to 100%), 63.5% (IQR 21.5% to 93.65%) and 51.7% (IQR 13.6% to 94.3%), 60.0% (IQR 10.0% to 95.1%) and 62.0% (IQR 0% to 100%), and 83.6% (IQR 73.3% to 90.7%) and 80.0% (IQR 70.3% to 87.8%) for BA, extent of ingrowth, BIC, extent of maximum depth, and deepest point in the equator and pole regions, respectively.

Similarly, no significant differences were found in terms of BA ( $p = 0.881$ ), extent of ingrowth ( $p = 0.710$ ), BIC ( $p = 0.626$ ), extent of maximum depth ( $p = 0.307$ ), and median deepest point ( $p = 0.361$ , all Mann-Whitney U test) between the equator and pole regions of the conventional implants. The median values were 34.1% (IQR 21.9% to 50.0%) and 33.8% (IQR 22.0% to 50.0%), 80.9% (IQR 56.5% to 100%) and 80.0% (IQR 53.9% to 100%), 20.0% (IQR 10.7% to 32.1%) and 20.0% (IQR 9.7% to 32.8%), 7.4% (IQR 0% to 31.6%) and 4.8% (IQR 0% to 29.2%), 59.7% (IQR 32.7% to 81.6%) and 59.3%

(IQR 32.7% to 79.1%) for BA, extent of ingrowth, BIC, extent of maximum depth, and deepest point in the equator and pole regions, respectively.

As expected, comparing the values measured in corresponding regions (equator or pole) between the two groups, significantly higher values were found for the 3D-printed implants ( $p < 0.001$ , Mann-Whitney U test). The distribution of the measured values for BA is shown in Figure 5b, divided according to the region (equator and pole).

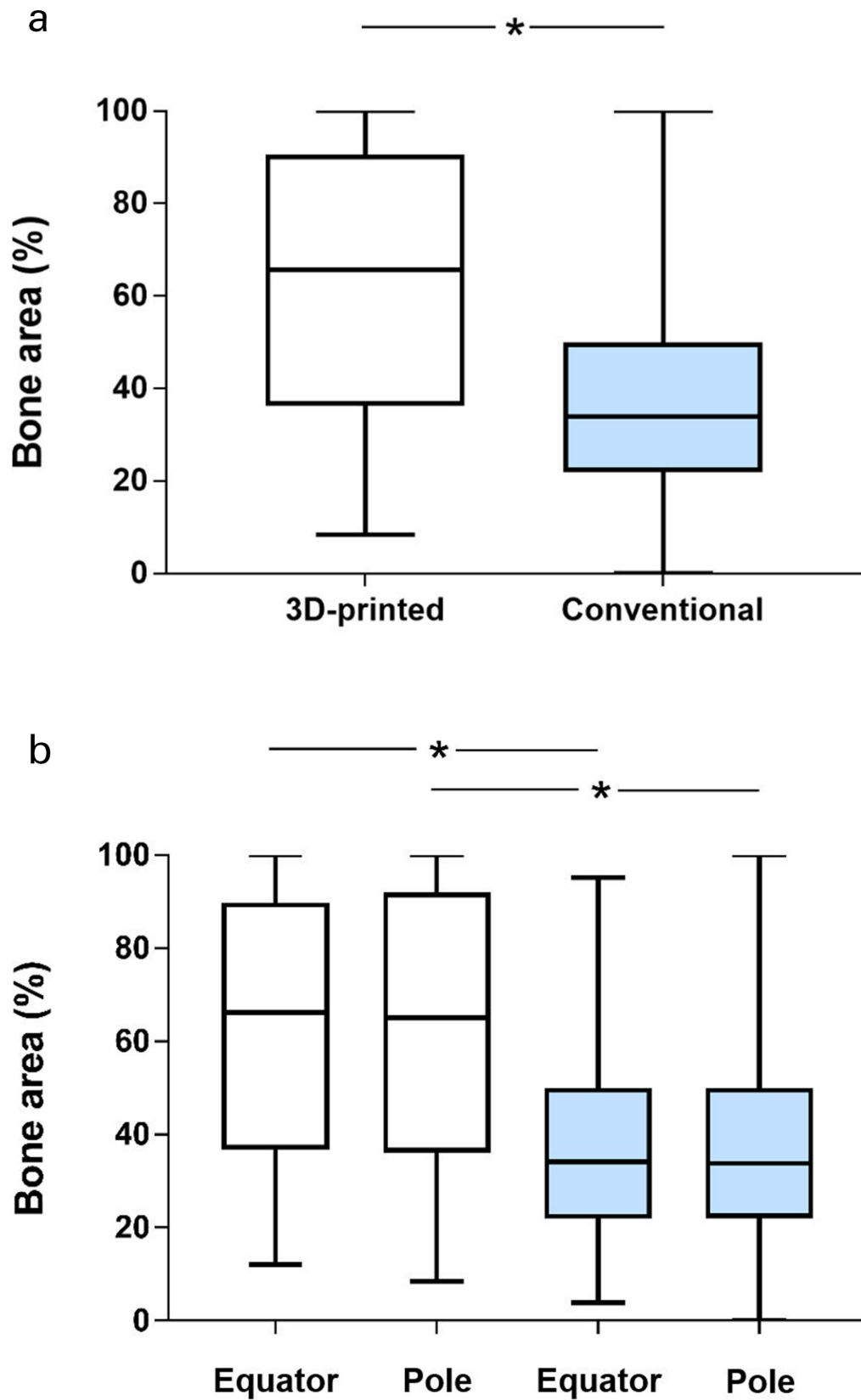
A comparison of the different implants within each group revealed a variability in the values measured for almost all the parameters representing bone ingrowth. This was true for all the bone integration parameters calculated for the 3D-printed group ( $p < 0.001$ ) and for all the parameters calculated for the conventional group ( $p < 0.001$ ) except the extent of ingrowth, where no statistically significant variability was found among the conventionally manufactured implants ( $p = 0.414$ , all Kruskal-Wallis test with post hoc Dunn's correction).

A summary of the values calculated for each individual acetabular implant is reported in Supplementary Table i.

## Discussion

This retrieval study was the first to investigate the extent of bone integration in retrieved 3D-printed acetabular implants, comparing them with conventionally manufactured highly porous acetabular implants. We found statistically significantly higher bone ingrowth in the 3D-printed implants than conventional, with almost double the amount of bone occupying the available porous space (63% to 37%), greater extent of bone presence across the backside surface (91% to 74%), and more than double BICs (56% to 26%) and extent of maximum depth reached by bone in the porous structure (52% to 19%). This suggested that 3D-printed implants may promote enhanced osseointegration, and this may be due to the possibility to create porous structures with optimal morphometric properties unique to 3D-printing technology.

The presence of lamellar bone in the 3D-printed implants, as well as in one of the conventional implants, suggests that the 3D-printed porous structure is able to promote a positive interaction with the host bone. The immature woven structure (non-mineralized



Box plots showing the distribution of the bone in growth values in terms of bone area, calculated for both a) the two whole groups and b) the specific regions within each group (equator, pole; white box plots for 3D-printed and blue for conventional). Statistically significant differences were found ( $*p < 0.001$ , Mann-Whitney U test).

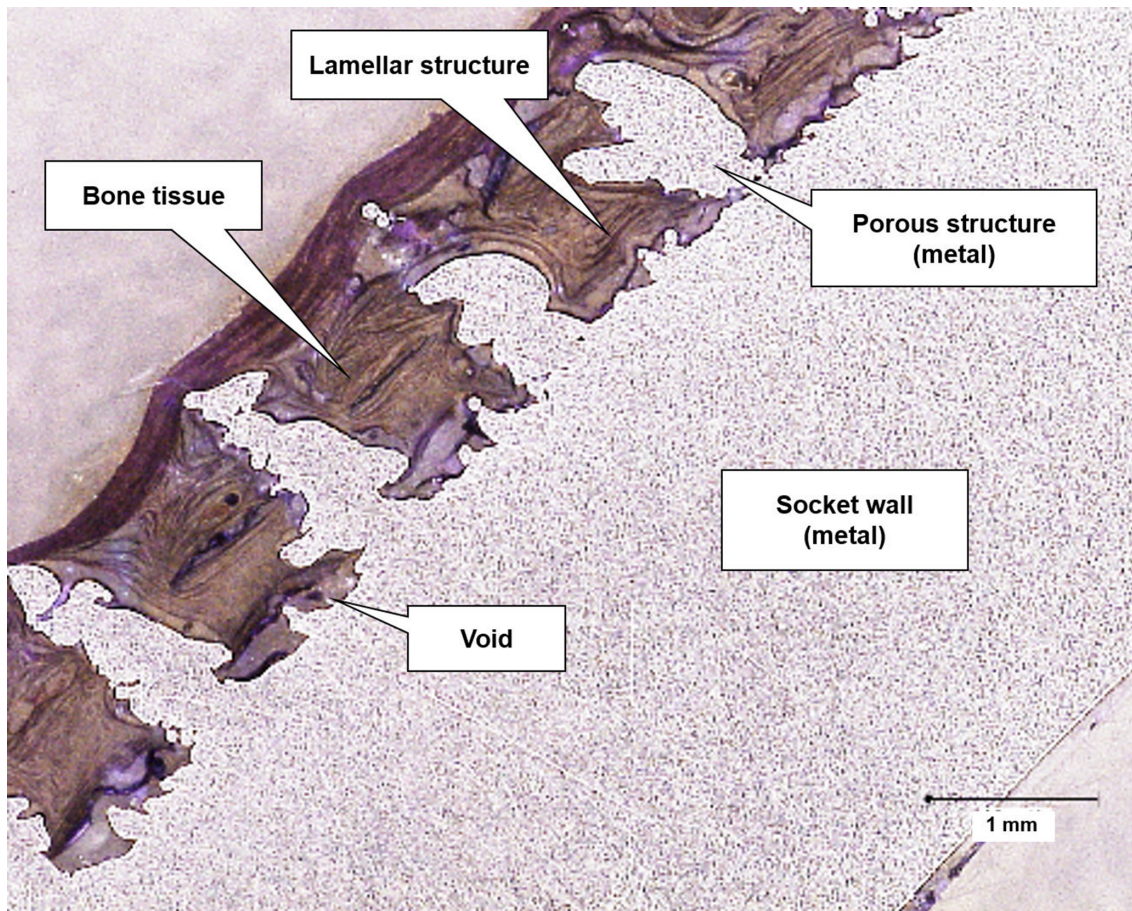


Fig. 6

Image captured from a histological section obtained from one of the 3D-printed implants; the lamellar structure of bone is visible. The different regions on the slice are specified (staining: Toluidine Blue, Paragon; magnification 50 $\times$ ).

disorganized collagen fibrils) is able to mature to a lamellar structure (collagen fibrils arranged in response to stresses), and this is only possible if bone cells encounter an artificial structure that promote osteogenic activity and subsequent remodelling process. Previous studies conducted on conventionally manufactured acetabular implants showed presence of lamellar bone near the rim (equator region) and adjacent to screw holes of implants retrieved after at least four to eight months of implantation.<sup>27,28</sup> It has been suggested that different factors may contribute to the maturation from woven to lamellar bone in porous implants, such as genetic factors, mechanical forces, and interaction between osteoblasts and osteoclasts.<sup>29</sup> The characteristics of the porous structure present on the 3D-printed implants analyzed may also be a contributing factor, given the specific porosity and pore size similar to those of cancellous bone (50% to 90%; ~ 1 mm)<sup>30</sup> and the thickness of the porous layer, which allowed an almost full penetration of bone, providing enough stability to promote bone tissue maturation. However, bigger

groups of 3D-printed implants are necessary to confirm these findings.

Considering the 3D-printed implants, a variability in the measured bone ingrowth parameters was found. This was not surprising, given that the specific clinical history of each patient (e.g. primary, revision, or re-revision surgery; bone quality) might have affected the degree of osseointegration. Overall, the BA fraction was in the range 25% to 96%, suggesting that the 3D-printed porous backside on the implants may promote satisfactory osseointegration to enable adequate fixation. Although lower values were reported for implants with a lower time to revision (16 months), the small number of implants analyzed could not allow the drawing of any conclusion in terms of correlation with this clinical parameter. However, it has been suggested that bone formation and osseointegration usually occur within eight to 12 weeks after surgery during the wound healing process,<sup>31</sup> thus suggesting that the implantation time may not be substantial.

It is interesting to note that one of the 3D-printed implants, despite being revised for infection after 50

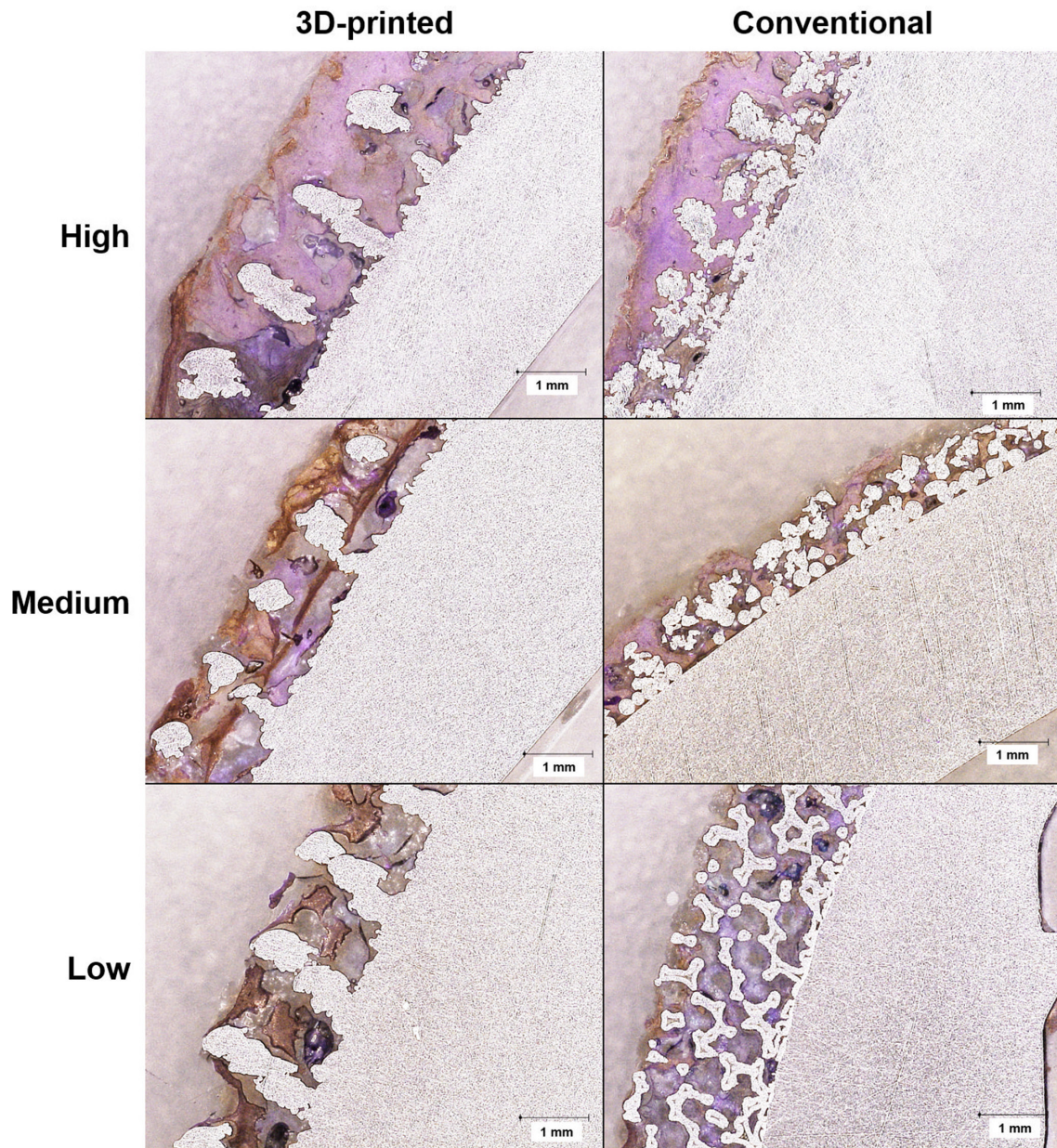


Fig. 7

Summary images taken from histological sections of both 3D-printed and conventional implants showing high, medium, and low percentages of bone ingrowth. For the conventional implants, the Tritanium, Gription, and Trabecular Metal porous structure layers are shown top to bottom (staining: Toluidine Blue, Paragon; magnification 50 $\times$ ).

months of implantation, showed good bone integration, thus suggesting that after the initial fixation, which is obtained by press-fitting the implant into an under-reamed acetabulum and potentially using screws, the secondary fixation, if reached, occurs in a relatively short time after implantation. Furthermore, the reason for revision of two of the 3D-printed implants in the study was reported as (aseptic) loosening. Both implants showed good amount of bone ingrowth, with mean BA fraction of 45% and 41% but a BIC of 37% and 15%, respectively, which are lower compared to the mean BIC of 67% exhibited by the other well-fixed implants. It has been

suggested that aseptic loosening may be due to poor BIC despite the presence of large amounts of bone within the implant porous structure as a result of distance osteogenesis rather than contact osteogenesis being the predominant mechanism.<sup>13</sup> 'Contact osteogenesis' is defined as the formation of bone tissue (through the action of bone matrix depositing osteoblasts) in an appositional fashion from the surface of the implant to the edge of the cut host bone, whereas 'distance osteogenesis' is regarded as the opposite mechanism, namely bone apposition from the cut host bone to the surface of the implant. The former has been suggested to be 30% faster than the latter.<sup>4,32</sup>

Thus, it can be speculated that the 3D-printed structure encouraged bone cell colonization and tissue proliferation at an early stage, which is confirmed by the time of implantation of these two 3D-printed implants (45.6 and 24.9 months), but this was not sufficient to prevent in situ micromotion which resulted in the loosening of the implants at a later stage. It has been demonstrated that micromotion of less than 100  $\mu\text{m}$  to 150  $\mu\text{m}$  may positively affect the osteoblasts' osteogenic activity, whereas higher values may be disruptive.<sup>33</sup> However, although the loosening of the implants may be considered a secondary event, it can be speculated that a successful osseointegration had not occurred in these two cases. It also needs to be added that the clinical history of one of these two implants included multiple revisions, which led the patient to receive a customized 3D-printed implant after revision of the off-the-shelf component, because of the poor bone conditions.

The 3D-printed acetabular design analyzed in this study was one of the first to be introduced in the market and it has been used in more than 100,000 hip arthroplasties worldwide. In 2018, this implant had been implanted in 13% of the revision cases using an uncemented acetabular implant performed in the UK (out of 3,799 uncemented acetabular implants used).<sup>1,25</sup> A clinical study related to this type of implant reported a survival rate of 95.6%, including both primary and revision cases, with satisfactory clinical and radiological outcomes, but was limited to short- to mid-term follow-up.<sup>5</sup> Although the relationship between bone ingrowth and clinical performance is still not fully understood, we demonstrated that 3D-printed implants may promote enhanced integration even in complicated cases, and together with the good clinical outcomes reported so far, this suggests that this type of implant can overcome some of the limitations shown by conventional implants.

The number of previous retrieval studies including acetabular implants for hip arthroplasty is limited and only includes conventionally manufactured implants. Hanzlik et al<sup>15</sup> analyzed bone ingrowth in acetabular implants coated with porous tantalum, reporting a mean bone volume fraction of 3.5% (standard deviation (SD) 1.5%; 1.2% to 6.9%), mean extent of ingrowth of 46% (SD 20%; 20% to 83%), and mean maximum depth reached by bone of 76% (SD 28%; 39% to 100%). In a more recent study, Baral et al<sup>17</sup> compared tantalum and fibre metal-coated implants, reporting mean volume fractions of 7% (SD 4%) and 21% (SD 17%), respectively. The tantalum acetabular implant included in our work exhibited a mean BA fraction of 30.6% (SD 16.1%; 9.5% to 70.7%), mean extent of ingrowth of 75.4% (SD 22.9%; 21.7% to 100%), and a mean maximum depth of ingrowth of 62.3% (SD 26.8%; 6.4% to 98.9%). The Trident I Tritanium implant showed a mean BA fraction of 49%, mean extent of ingrowth of 78%, and mean BIC of 41%. This design has been implanted in 16% (out of 3,799) of the uncemented acetabular revisions performed in the UK in 2018;<sup>1</sup> satisfactory mid-term clinical outcomes have been

reported, with a survivorship of 97.9% at five years.<sup>1,5</sup> The R3 StikTite implants exhibited mean BA fraction of 31%, mean extent of ingrowth of 72%, and mean BIC of 19%. This design has implanted in 8% (out of 67,514) of the uncemented acetabular primary procedures performed in the UK in 2018;<sup>1</sup> survivorship of 97.1% at five years has also been reported.<sup>34</sup> The Pinnacle Gription implant showed mean BA fraction of 41%, mean extent of ingrowth of 73%, and mean BIC of 27%. This design was used in 13% (out of 3,799) of the uncemented acetabular revisions performed in the UK in 2018<sup>1</sup>; short-term clinical outcomes revealed a 95.8% survivorship at 43.5 months follow-up.<sup>35</sup>

Overall, the differences in bone ingrowth between the two groups are not reflected in the clinical outcomes, which have been reported to be positive for both 3D-printed and highly porous conventionally manufactured uncemented acetabular implants. This suggests that the amount of bone ingrowth is important, but not the only factor in determining successful clinical outcomes. However, morphometric features of the porous structure such as porosity and pore size are key parameters to determine the integration performance of the implant. The 3D-printing manufacturing technology enables a better design of these features, optimizing the amount and location of metal and therefore generating a pre-defined optimal porous structure for bone ingrowth.<sup>3,26</sup> This may be one of the main factors contributing to a better osseointegration of this type of implant compared to conventional counterparts.

This study had several limitations. First, the small number of implants analyzed. It is recognized that the retrospective analysis of failed implants is underperformed because of the limited number of retrieved implants, and logistical issues such as preservation, storage, and transportation of the retrieved clinical material, with the added unlikelihood of there being comparable inter-patient clinical conditions, as shown in a previous retrieval study.<sup>36</sup> Furthermore, it cannot be excluded that the area of bone ingrowth to the available bone fixation surface may have been reduced by macrophage activity in the metal-on-metal designs included in the study.

Another limitation is related to the heterogeneity of the groups, in terms of reasons of revisions and implant designs. The rationale behind this choice is that all the implants included in our study were "highly porous", and their primary clinical purpose was to promote enhanced osseointegration. Future studies will focus on specific designs, reducing such variability. Several confounding variables related to individual patients might have affected the reported outcomes. Surgeon, patient, and implant factors such as the quality of surgery, patients' demographics and habits, or factors influencing the bone quality, such as the presence of bone poisoned by metal debris, need to be taken into account. In particular, bone quality is a key factor that needs to be considered, because the implant has to provide the environment suitable for osseointegration, but the host bone (after the

surgical preparation, which may leave a poor bone stock especially in case of multiple revision surgeries) needs to be able to interact with the structure of the implant and integrate with it. The two groups considered in this study were matched for the majority of characteristics related to these factors (age, time to revision, sex, and implant size), which might have partially overcome such limitations. Overall, we analyzed a meaningful cohort that was representative of the implants currently used in clinical practice.

In conclusion, this was the first study to investigate the osseointegration of 3D-printed acetabular implants retrieved from patients. The null hypothesis that the manufacturing method (3D-printing or conventional) has no effect on the implant-bone integration had to be rejected. A higher degree of bone ingrowth was found in the 3D-printed implants, suggesting that enhanced osseointegration can be achieved with this type of implant.

Further studies including a greater number of implants and different 3D-printed acetabular designs will help to provide more evidence on the clinical performance of these types of orthopaedic implants.

### Supplementary material



Table showing values for bone ingrowth parameters measured for each individual implant included in the study.

### References

- No authors listed.** 16th annual report. National Joint Registry for England, Wales, Northern Ireland and the Isle of Man. 2019. <https://reports.njrcentre.org.uk/portals/0/pdfdownloads/njr%2016th%20annual%20report%202019.pdf> (date last accessed 9 June 2021).
- Dall'Ava L, Hothi H, Di Laura A, Henckel J, Hart A.** 3D Printed Acetabular CUPS for Total Hip Arthroplasty: A Review Article. *Metals (Basel)*. 2019;9(7):729.
- Lowther M, Louth S, Davey A, et al.** Clinical, industrial, and research perspectives on powder bed fusion additively manufactured metal implants. *Additive Manufacturing*. 2019;28(780):565–584.
- Goriainov V, Cook R, M Latham J, G Dunlop D, Oreffo ROC.** Bone and metal: an orthopaedic perspective on osseointegration of metals. *Acta Biomater*. 2014;10(10):4043–4057.
- Malahias M-A, Kostretzis L, Greenberg A, Nikolaou VS, Atrey A, Sculco PK.** Highly porous titanium acetabular components in primary and revision total hip arthroplasty: a systematic review. *J Arthroplasty*. 2020;35(6):1737–1749.
- Benazzo F, Botta L, Scaffino MF, et al.** Trabecular titanium can induce in vitro osteogenic differentiation of human adipose derived stem cells without osteogenic factors. *J Biomed Mater Res A*. 2014;102(7):2061–2071.
- Van Bael S, Chai YC, Truscetto S, et al.** The effect of pore geometry on the in vitro biological behavior of human periosteum-derived cells seeded on selective laser-melted Ti6Al4V bone scaffolds. *Acta Biomater*. 2012;8(7):2824–2834.
- Taniguchi N, Fujibayashi S, Takemoto M, et al.** Effect of pore size on bone ingrowth into porous titanium implants fabricated by additive manufacturing: an in vivo experiment. *Mater Sci Eng C Mater Biol Appl*. 2016;59(176):690–701.
- Tanzer M, Chuang PJ, Ngo CG, Song L, TenHuisen KS.** Characterization of bone ingrowth and interface mechanics of a new porous 3D printed biomaterial: an animal study. *Bone Joint J*. 2019;101-B(6\_Suppl\_B):62–67.
- Ragone V, Canciani E, Arosio M, et al.** In vivo osseointegration of a randomized trabecular titanium structure obtained by an additive manufacturing technique. *J Mater Sci Mater Med*. 2020;31(2):17.
- Ruppert DS, Harrysson OLA, Marcellin-Little DJ, Abumoussa S, Dahners LE, Weinhold PS.** Osseointegration of Coarse and Fine Textured Implants Manufactured by Electron Beam Melting and Direct Metal Laser Sintering. *3D Print Addit Manuf*. 2017;4(2):91–97.
- Palmquist A, Shah FA, Emanuelsson L, Omar O, Suska F.** A technique for evaluating bone ingrowth into 3D printed, porous Ti6Al4V implants accurately using X-ray micro-computed tomography and histomorphometry. *Micron*. 2017;94:1–8.
- Shah FA, Thomsen P, Palmquist A.** Osseointegration and current interpretations of the bone-implant interface. *Acta Biomater*. 2019;84:1–15.
- Swarts E, Bucher TA, Phillips M, Yap FH.** Does the ingrowth surface make a difference? A retrieval study of 423 cementless acetabular components. *J Arthroplasty*. 2015;30(4):706–712.
- Hanzlik JA, Day JS, Klein GR, Levine HB, Hartzband MA, Parvizi J, Acknowledged Contributors: Ingrowth Retrieval Study Group.** Bone ingrowth in well-fixed retrieved porous tantalum implants. *J Arthroplasty*. 2013;28(6):922–927.
- Urban RM, Hall DJ, Della Valle C, Wimmer MA, Jacobs JJ, Galante JO.** Successful long-term fixation and progression of osteolysis associated with first-generation cementless acetabular components retrieved post mortem. *J Bone Joint Surg Am*. 2012;94-A(20):1877–1885.
- Baral EC, Trivellas M, Vigdorichik JM, Ricciardi BF, Wright TM, Padgett DE.** Porous coatings in retrieved acetabular components. *J Arthroplasty*. 2020;35(8):2254–2258.
- Beckmann NA, Bitsch RG, Gondon M, Schonhoff M, Jaeger S.** Comparison of the stability of three fixation techniques between porous metal acetabular components and augments. *Bone Joint Res*. 2018;7(4):282–288.
- Beckmann NA, Jaeger S, Janoszka MB, Klotz MC, Bruckner T, Bitsch RG.** Comparison of the primary stability of a porous coated acetabular revision cup with a standard cup. *J Arthroplasty*. 2018;33(2):580–585.
- Banerjee S, Issa K, Kapadia BH, Pivec R, Khanuja HS, Mont MA.** Systematic review on outcomes of acetabular revisions with highly-porous metals. *Int Orthop*. 2014;38(4):689–702.
- Hothi H, Dall'Ava L, Henckel J, et al.** Evidence of structural cavities in 3D printed acetabular CUPS for total hip arthroplasty. *J Biomed Mater Res B Appl Biomater*. 2020;108(5):1779–1789.
- Hothi HS, Berber R, Whittaker RK, Bills PJ, Skinner JA, Hart AJ.** Detailed inspection of metal implants. *Hip Int*. 2015;25(3):227–231.
- Chan O, Coathup MJ, Nesbitt A, et al.** The effects of microporosity on osteoinduction of calcium phosphate bone graft substitute biomaterials. *Acta Biomater*. 2012;8(7):2788–2794.
- DeLee JG, Charnley J.** Radiological demarcation of cemented sockets in total hip replacement. *Clin Orthop Relat Res*. 1976;121:20–32.
- Dall'Ava L, Hothi H, Henckel J, Di Laura A, Shearing P, Hart A.** Comparative analysis of current 3D printed acetabular titanium implants. *3D Print Med*. 2019;5(1):15.
- Dall'Ava L, Hothi H, Henckel J, Di Laura A, Shearing P, Hart A.** Characterization of dimensional, morphological and morphometric features of retrieved 3D-printed acetabular CUPS for hip arthroplasty. *J Orthop Surg Res*. 2020;15(1):1–12.
- Sumner DR, Jasty M, Jacobs JJ, et al.** Histology of porous-coated acetabular components. 25 cementless CUPS retrieved after arthroplasty. *Acta Orthop Scand*. 1993;64(6):619–626.
- Pidhorz LE, Urban RM, Jacobs JJ, Sumner DR, Galante JO.** A quantitative study of bone and soft tissues in cementless porous-coated acetabular components retrieved at autopsy. *J Arthroplasty*. 1993;8(2):213–225.
- Frosch K-H, Barvencik F, Lohmann CH, et al.** Migration, matrix production and lamellar bone formation of human osteoblast-like cells in porous titanium implants. *Cells Tissues Organs*. 2002;170(4):214–227.
- Keaveny TM, Morgan EF, Niebur GL, Yeh OC.** Biomechanics of trabecular bone. *Annu Rev Biomed Eng*. 2001;3(1):307–333.
- Cook SD, Barrack RL, Thomas KA, Haddad RJ.** Quantitative analysis of tissue growth into human porous total hip components. *J Arthroplasty*. 1988;3(3):249–262.
- Puleo DA, Nanci A.** Understanding and controlling the bone-implant interface. *Biomaterials*. 1999;20(23–24):2311–2321.
- Ziebart J, Fan S, Schulze C, Kämmerer PW, Bader R, Jonitz-Heincke A.** Effects of interfacial micromotions on vitality and differentiation of human osteoblasts. *Bone Joint Res*. 2018;7(2):187–195.
- Wilson IR, Turgeon TR, Gascoyne TC, Della Valle CJ, McCalden RW.** Midterm Results of a Contemporary, Porous-Coated Acetabular System in Patients Undergoing Primary Total Hip Replacement for Degenerative Hip Disease: A Prospective, Multicenter Study. *J Arthroplasty*. 2020;35(7):1862–1867.
- Chacko V, Agrawal P, Porter ML, Board TN.** Early results of a high friction surface coated uncemented socket in revision hip arthroplasty. *Hip Int*. 2020;30(6):739–744.
- Panagiotopoulou VC, Davda K, Hothi HS, et al.** A retrieval analysis of the Precice intramedullary limb lengthening system. *Bone Joint Res*. 2018;7(7):476–484.

**Author information:**

- L. Dall'Avà, BEng, MSc, PhD, Researcher, Institute of Orthopaedics and Musculoskeletal Science, Division of Surgery and Interventional Science, University College London, Stanmore, UK.
- H. Hothi, BEng, MSc, PhD, Implant Science Fellow
- J. Henckel, MD, Orthopaedic Surgeon
- A. Di Laura, BEng, MSc, PhD, Senior Researcher
- J. Skinner, MB, BS, FRCS(Eng), FRCS(Orth), Consultant Orthopaedic Surgeon and Director of Research and Innovation Centre  
Royal National Orthopaedic Hospital NHS Trust, Stanmore, UK.
- R. Tirabosco, MD, Consultant Histopathologist, Department of Histopathology, Royal National Orthopaedic Hospital NHS Trust, Stanmore, UK.
- A. Eskelinen, MD, PhD, Chief Orthopaedic Surgeon and Research Director, The Coxa Hospital for Joint Replacement, Tampere, Finland.
- A. Hart, MA, MD, FRCS(Orth), Professor of Orthopaedic Surgery, Consultant Orthopaedic Surgeon and Director of Research for Implant Science, Institute of Orthopaedics and Musculoskeletal Science, Division of Surgery and Interventional Science, University College London, Stanmore, UK; Royal National Orthopaedic Hospital NHS Trust, Stanmore, UK.

**Author contributions:**

- L. Dall'Avà: Conceptualized and designed the study, Acquired, analyzed, and interpreted the data, Drafted and critically revised the manuscript.
- H. Hothi: Conceptualized and designed the study, Acquired, analyzed, and interpreted the data, Drafted and critically revised the manuscript.
- J. Henckel: Conceptualized and designed the study, Acquired, analyzed, and interpreted the data, Drafted and critically revised the manuscript.
- A. Di Laura: Conceptualized and designed the study, Critically revised the manuscript.
- R. Tirabosco: Analyzed and interpreted the data.
- A. Eskelinen: Conceptualized and designed the study, Critically revised the manuscript.
- J. Skinner: Conceptualized and designed the study.
- A. Hart: Conceptualized and designed the study, Acquired, analyzed, and interpreted the data, Drafted and critically revised the manuscript.

**Funding statement:**

- This research did not receive any specific grant from funding agencies in the public, commercial, or not-for-profit sectors. No conflict of interests related to this publication were present. No benefits in any form have been received or will be received from a commercial party related directly or indirectly to the subject of this article.

**ICMJE COI statement:**

- A. Hart reports institutional grants (paid to University College London) from LimaCorporate and DePuy Synthes, and consultancy fees from DePuy Synthes, all unrelated to this study. These grants were provided from LimaCorporate for work on the clinical outcome of custom implants, and from DePuy Synthes for the storage of metal-on-metal hip implants.
- A. Eskelinen reports institutional grants (paid to The Coxa Hospital for Joint Replacement) from DePuy Synthes and Zimmer Biomet, and lecture fees from Zimmer Biomet, all unrelated to this study.

**Acknowledgements:**

- This research study was supported by The Maurice Hatter Foundation, the Royal National Orthopaedic Hospital (RNOH) Charity, the Rosetrees Trust, and the Stonegate Trust, and was supported by researchers at the National Institute for Health Research University College London Hospitals Biomedical Research Centre.

**Ethical review statement:**

- We confirm that all investigations were conducted in conformity with ethical principles of research, that informed consent for participation in the study was obtained, and that institutional approval of the human protocol for this investigation was obtained (London-Riverside REC 07/Q0401/25).

**Open access funding:**

The authors report that they received open access funding for their manuscript from the institutional fund of University College London.

© 2021 Author(s) et al. Open Access This article is distributed under the terms of the Creative Commons Attribution (CC BY 4.0) licence (<https://creativecommons.org/licenses/by/4.0/>), which permits unrestricted use, distribution, and reproduction in any medium or format, provided the original author and source are credited.